DOI: 10.1007/s11427-006-2015-0

Remote sensing and geographic information systems in the spatial temporal dynamics modeling of infectious diseases

GONG Peng [1], XU Bing [2] & LIANG Song [1, 3]

1. State Key Laboratory of Remote Sensing Science, Jointly Sponsored by the Institute of Remote Sensing Applications, Chinese Academy of Sciences and Beijing Normal University, Box 9718, Beijing 100101, China;
2. Department of Geography, University of Utah, Salt Lake City, UT 84112, USA;
3. School of Public Health, University of California, Berkeley, CA 94720, USA

Correspondence should be addressed to Gong Peng (email: gong@irsa.ac.cn)

Received March 14, 2006; accepted June 29, 2006

Abstract Similar to species immigration or exotic species invasion, infectious disease transmission is strengthened due to the globalization of human activities. Using schistosomiasis as an example, we propose a conceptual model simulating the spatio-temporal dynamics of infectious diseases. We base the model on the knowledge of the interrelationship among the source, media, and the hosts of the disease. With the endemics data of schistosomiasis in Xichang, China, we demonstrate that the conceptual model is feasible; we introduce how remote sensing and geographic information systems techniques can be used in support of spatio-temporal modeling; we compare the different effects caused to the entire population when selecting different groups of people for schistosomiasis control. Our work illustrates the importance of such a modeling tool in supporting spatial decisions. Our modeling method can be directly applied to such infectious diseases as the plague, lyme disease, and hemorrhagic fever with renal syndrome. The application of remote sensing and geographic information systems can shed light on the modeling of other infectious disease and invasive species studies.

Keywords: spatio-temporal modeling, spatial connectivity, prevention and control of infectious diseases, biological invasion.

1 Introduction

Infectious disease dispersion is becoming more rapid and more extensive due to economic globalization. The impact of infectious diseases is often related to the population of the entire world. Severe Acute Respirotory Syndrome (SARS) rapidly spread over 30 countries and regions during a period of less than half a year from the beginning of 2003, leading to over 8000 infected people and over 700 deaths(http://www.cdc.gov/ncidod/sars/). The West Nile virus, originating from Uganda, was found in New York in 1999, and had spread to over 44 states by 2002; in 2003 and 2004, the West Nile virus had infected over 12000 people, killing 350(http://www.cdc.gov/ncidod/dvbid/westnile/). After battling schistosomiasis for many years along the Yangtze River Basin, many counties in China had the disease under control for some time. However, there have been recent resurgences in many counties. In 2004, seven counties that used to have schistosomiasis under control had resurgences of the disease.

The factors that dominate the spreading mechanism of a particular infectious disease are still unknown. For example, though the direct reason of SARS dispersal is due to human air travel, we have little understanding of its origin, transmission channel, and media. However, many other diseases are being carried around spatially by trade and tourism, but do not spread in their new environment. Therefore, we would like to ask which diseases will be spread around the globe successfully via globalization. What are their origins, destinations, and spreading channels? What is the likelihood of survival and endemics of a pathogen under new environment?

In order to answer those questions, we need to develop models that can predict the transmission of infectious diseases. We need to understand the history and current endemic region of an infectious disease. There are three stages in predicting the transmission of infectious diseases: (1) identification of the pathogen, its animal host, and its pathway of transmission among the hosts; (2) determining the spatial transmission pattern of each infectious disease, particularly the relationship between the distribution of the disease and its environment; (3) understanding the dynamic process of the transmission of the disease, using models calibrated with field survey data[1]. The epidemiological model thus established will have the capability to predict the dispersal of the virus, and its likelihood of transmission in new environment. However, each of these stages is difficult to complete. The work at stage one is a diagnosis and initial exploration of the disease. For a new virus, there is the possibility of important new discoveries.

The second stage involves the survey and quantitative description of the spatial and temporal pattern of an infectious disease, followed by an analysis of the relationship of the disease with its environment. Geographic information systems (GIS), remote sensing, and statistical methods are most suitable to deal with the problems at this stage. Remotely sensed data provide us with information about the land cover, surface temperature, soil moisture, and vegetation growth. Such information is very useful in indirectly predicting the abundance of virus transmission vectors, including mosquitoes, ticks, mice and snails. GIS provides a spatial database containing environmental and epidemiological data. Such data provide a basis for statistical analysis. For example, with GIS one can explore the statistical relationship between infectious disease data and environmental data, and then map the risk level in the area of interest. Infection risk mapping is usually based on environmental suitability analysis. This is done by searching for the environment whose conditions meet the requirement of a particular infectious disease. There are four cases that can result from the comparison between suitability for and actual distribution of a particular disease: first, the actual distribution is located in the suitable area; second, the disease is found in unsuitable areas; third, the suitable area does not have the actual disease. Though the first and second cases are the most reasonable ones, the third should not be considered incorrect. Only when the distribution area is classified as an unsuitable area, is the third case incorrect. More can be done with GIS. For example, when examining the infection risk distribution of schistosomiasis, one can evaluate the spatial autocorrelation among different residential groups; such information is helpful in the spatial control of the disease transmission[2,3]

The third stage is based on the two previous stages. The goal is to establish a quantitative process based biological model. Such models can be calibrated with field measurements and surveys. In general, these models are limited to modeling the biological reproduction cycle of a particular disease, and relevant hosts[4]. However, there are also studies that directly model the dynamics between the environment and the transmission vector. For example, the relationship between the climate and mosquito populations can be modeled. Rogers and Randolph[1] found that the surface temperature is nonlinearly related to the mortality of Gambia TseTse Fly with a one-month time lag.

We are certain that the increase of spatial connectivity and environmental change resulting from globalization are two dominant reasons for the intensification of the spread of infectious diseases. Similar to invasive species, there exists a positive feedback between the intensification of infectious diseases and environmental change (Fig. 1). GIS and remote sensing are important tools for the study of spatial connectivity and environmental change, respectively.

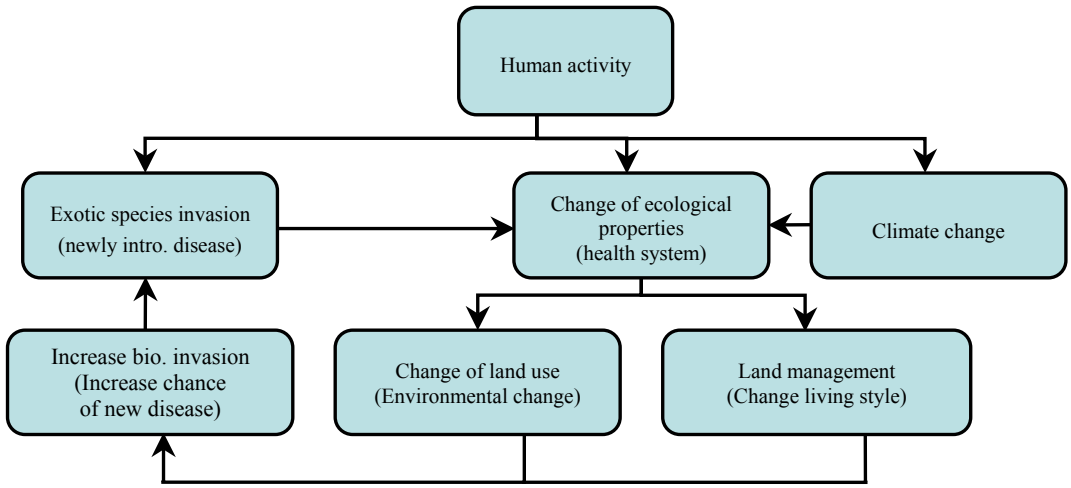

Fig. 1. The relationship between the invasion of exotic species and environmental change. Human activities cause the migration of species, changes in ecological properties, and climate changes (mainly through modification of atmospheric constituents). Climate change and species migration may alter the ecological condition of a new area. Faced with changes in ecological conditions, humans may alter their land use and land management in order to protect themselves. Any of these behaviors would cause new invasions. This positive feedback model equally suits the introduction and dispersion of infectious diseases.

It is worth mentioning that the three stages of study are usually independently undertaken. It is particularly true for the second and third stages. This has largely limited the understanding of the impact of the environment on the transmission of infectious diseases. Such a limitation further hampers disease control and prevention. In this paper, we use schistosomiasis as an example to illustrate the important roles that remote sensing and GIS can play in modeling the interaction between the environment and disease transmission.

2 A conceptual mathematical model of the life cycle of schistosomiasis

According to the World Health Organization, schistosomiasis disease is endemic in 74 countries with approximately 120 million people infected and over 600 million people at risk. In China, there are approximately 800,000 people infected and over 60 million at risk. In recent years, the patterns of endemic occurrences and control of schistosmiasis have been changing due to changes in social-economic and natural factors. On the one hand, some endemic areas have intensified the risk of schistosomiasis infection. On the other hand, some areas that were not endemic areas in the past, for example, in the mountainous areas of Sichuan Province, where snails are present but have had no historically reported schistosomiasis infection, have become endemic areas. How and where new snail habitats will emerge according to recent environmental changes have increasingly attracted research attention.

Our model is obtained by adding a spatial connectivity component, and simplifying the temporal dynamics from a detailed dynamics model by Liang *et al*.[5]. According to the life cycle of schistosomiasis in Fig. 2, we can build the above conceptual model. We first describe the number of adult worms in the final host as a function of time

$$\frac{dW_i}{dt} = \beta_i c_i - \mu_w W_i - \pi_i W_i, \tag{1}$$

where W_i is the worm load in village i (or country, or group of human, or cattle) at time t; β_i is the infection rate through water contamination with cercaria (density c_i); μ_w is the natural death rate of schistosome in the host; π_i is the death rate of schistosomes by medical treatment. In the life cycle, egg production by unit time is modeled by

$$e_i = \frac{1}{2} h g n_i W_i \phi, \tag{2}$$

where e_i is the average egg production of n_i infected people in group i. Half of the adult worms produce eggs of quantity h, produced by each worm. The

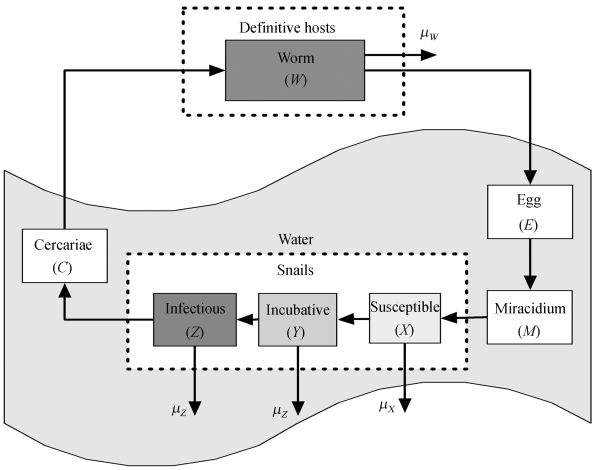

Fig. 2. The life cycle of schistosomiasis. Egg (*E*) are excreted with the stool of humans and other animal hosts (i.e. water buffalo and other cattle). They then hatch into miracidia, *M*, in water with suitable temperature. Miracidia must penetrate into snails within 48 h in the water, causing the susceptible snails, *X*, to be infected into *Y*. The incubation of the miracidia will last 30—60 d to asexually reproduce into cercaria, *C*. The number of infected snails that survive to this stage are noted as *Z*. Cercaria must penetrate the skin of their final host in the water within 48 hours and find their final destination near the liver organ of the host and grow into the adult schistosome, *W*, where they pair to reproduce eggs and complete the life cycle. Human and cattle get infected by schistosomiasis through contact with contaminated water by cercaria (e.g. work in the field, grazing, washing, swimming, etc.).

number of eggs contained in each gram of stool is *g*. Because the life cycle of the adult worm is longer than the other forms, we will not use a differential equation to model the number of eggs. The successfully hatched eggs into miracidia are determined by

$$m_i = \sum_{j=1}^{n} \frac{\alpha e_j S_{ij}}{b_i}, \tag{3}$$

where m_i is the density of miracidia in group i, which includes the import and export of miracidia from other groups; the hatching rate is α and the area of water surface is b_i; the redistribution coefficient among neighboring groups is S_{ij}; n represents the number of groups. The key to the spatial dispersion of schistosomes is to determine the spatial distribution coefficients as a function of the spatial interaction at different levels. This is determined by the spatial interaction processes at different scales. In general, a hierarchical scheme is needed to construct the spatial distribution coefficient. Because we lack the spatial interaction data at multiple scales, we only use a distance (e.g., 1.5 km) to determine the interconnection among neighboring groups through the ditch networks. This is done with GIS (see the next section). The infection of snails by miracidia in the water is de- scribed by

$$\frac{dZ_i}{dt} = \rho m_i x_i - \mu_z Z_i, \tag{4}$$

where Z_i is the number of infected snails that are shedding cercaria; this is determined by the total snail density, x_i, and the density of miracidia, m_i, the infection rate of snails, ρ, and the death rate of snails, μ_z. Snail density, x_i is obtained with remote sensing methods (see section 4). Finally, the cercaria production is determined by

$$c_i = \sum_{j=1}^{n} \frac{\sigma Z_j a_j S_{ij}}{b_i}, \tag{5}$$

where σ is the daily cercaria production rate of each infected snail; a_j is the water area of snail habitat. The above model omitted the infected latent snail, *Y*, as shown in Fig. 2. To obtain *Z* from *Y*, one only needs to multiply with a death rate of infected snails. The above 5 equations provide us with a spatio-temporal model for schistosomiasis transmission. .

The model described above is based on the following assumptions: (1) the accessible and associated immunization among host groups during the infection process is ignored; (2) there is no density dependence in schistosomiasis infection, this assumption is reasonable when the modeling period is not long (~5 years); (3) there is no relationship between the number of miracidia that infect snails and the number of cercaria shed by infected snails; (4) the aggregation distribution parameter, *k*, in host groups is constant;(5) the host population during the modeling process is constant; (6) annual climate change does not change (although the model can accommodate climate change with available data). Values for each parameter in this model are listed in Table 1.

3 Spatial interaction determination between neighboring villages through GIS

We selected an endemic area of schistosomiasis in Xichang surrounding Qionghai Lake for our study area. The area has 227 natural villages covered by one scene of IKONOS imagery(11 km×11 km)(27°47′—27°50′N, 102°14′—102°18′E)(Fig. 3), and is located in the western mountainous area in Sichuan Province at an

Table 1 Parameter ranges in the schistosomiasis transmission model

Parameter	Interpretation and unit	Range	Reference
τ_w	development time of worms in human hosts (day)	20－40	[4]
μ_w	worm natural mortality (/day)	0.000183－0.0014	[4]
h	eggs excreted (/worm pair /gram feces)	0.768－2.72	[6]
μ_s	snail mortality rate (/day)	0.0023－0.007	[7]
μ_z	patent and latent snail death rate (/day)	0.0063－0.033	[8]
π_i	efficacy of praziquantel	0.8－0.95	[9, 10]
σ	cercarial production (/sporocyst/day)	20－50	[11, 12]
β	schistosome infection rate (/cercaria/m^2 contact)	0.0001－0.5	model calibration
ρ	snail infection (/miracidium/m^2 surface water)	0.000001－0.0005	model calibration
w_{0i}	initial worm burden in the ith group	data estimated	local data
z_0	initial density of infected snails	data estimated	local data & satellite image
x_0	initial density of susceptible snails	data estimated	local data & satellite image
κ_{0i}	initial worm aggregation parameter	data estimated	local data

Distributions for all parameters are uniform except for α and ρ, which have log-uniform distributions.

elevation between 1500 m and 2700 m. We constructed a digital elevation model (DEM) based on a stereopair of ASTER images acquired in August of 2002 with a grid size of 15 m (Fig. 4). The precision of this DEM is assessed by taking GPS measurements of 29 points in the study area, resulting in an average error of less than 6 m. This level of accuracy is sufficient for our analysis.

We digitized the boundaries of 227 villages, and inputted them into a GIS database. In the GIS, we calculated the geometric center of each natural village,

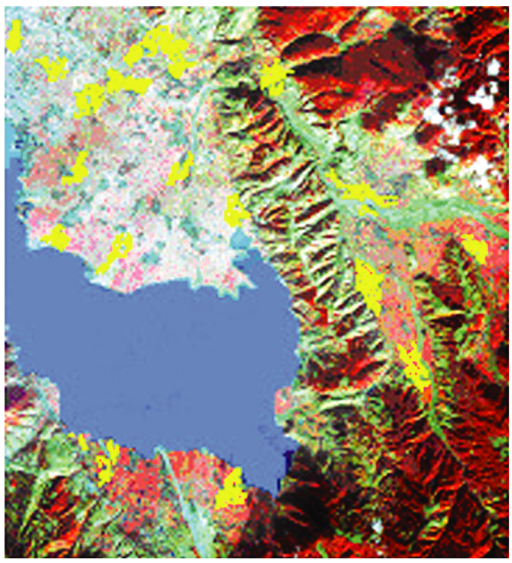

Fig. 3. The IKONOS image of Xichang acquired in December of 2000. The false color image is made from a combination of green, red and near infrared bands displayed with a color gun of blue, green and red, respectively. The yellow areas are the ditches where field snail surveys were conducted in 19 villages.

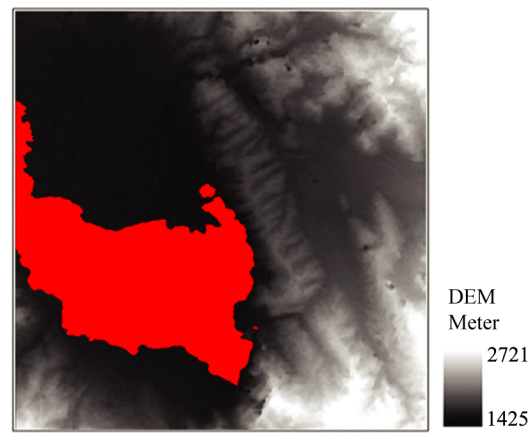

Fig. 4. The digital elevation model of the study area derived from a stereopair of ASTER images. The red area is the Qionghai Lake extracted from image analysis of the image in Fig. 3.

and then calculated the inter-distance among the neighboring villages. We also calculated the number of neighboring villages for each village. With the boundaries of the natural villages overlaid on top of the DEM, we calculated the average elevation for each village. The slope between the center points and the direction of ditch water flow between the neighboring villages was determined by comparing the average elevation between neighboring villages. The amount of miracidia and cercaria exchange and retention was determined by water flow direction, slope between neighboring villages, and the area of each individual village. Miracidia and cercaria flowed in the direction of the water flow. Therefore, only villages at lower elevations received inputs from villages at higher ele-

vations.

We constructed a village-to-village spatial connection matrix S. The ith row and jth column, S_{ij}, represents the number of miracidia and cercaria transport from the ith village to the jth village. In this study we did not consider the migration of snails and eggs, because the active movement of snails is rather limited in space, and the eggs stored in stool are mostly accumulated by individual farmers and applied to their own fields near their house. The interaction of eggs between neighboring villages is limited. Passive movement of snails is usually caused by the transport of agricultural products, but their numbers are usually low. Therefore, we ignored this. The diagonal elements in S represent the retention rates of the villages. The retention rate, S_{ii}, is related to the area and slope of the village. The calculation was done by setting an upper and lower bound (0.3—0.9), and by building a linear model of slope and area. The retention rate was then calculated as the average between the outcomes of the slope function and area function. The Sichuan Institute of Parasitic Diseases conducted some observations of the viability of cercaria and miracidia with respect to the hydrological condition in the study area, finding that their distance of movement during half of a lifetime in water was 400 m. However, the average diameter of natural villages is 500 m. Therefore, we did not consider indirectly connected villages. Clearly, S is not symmetric. If $S_{ij}>0$ then $S_{ji} = 0$, because miracidia and cercaria can only flow from higher places to lower places. S_{ij} is estimated by

$$S_{ij} = (1 - S_{ii})\omega_j,$$
$$\omega_j = \beta_{ij} / \sum_{k=1}^{ne} \beta_{ik}, \quad (6)$$

where ne represents the effective neighbors of the ith village, that is, those villages having a higher elevation than village i; β is the slope; and ω is the normalization factor.

Applying the above method, we can get the spatial interaction matrix as displayed in Fig. 5. Substituting S_{ij} into eqs. (3) and (5) allows us to redistribute the iracidia and cercaria numbers among the 227 villages. Xu *et al*.[13] introduced a simpler version of this spatial interaction matrix construction method.

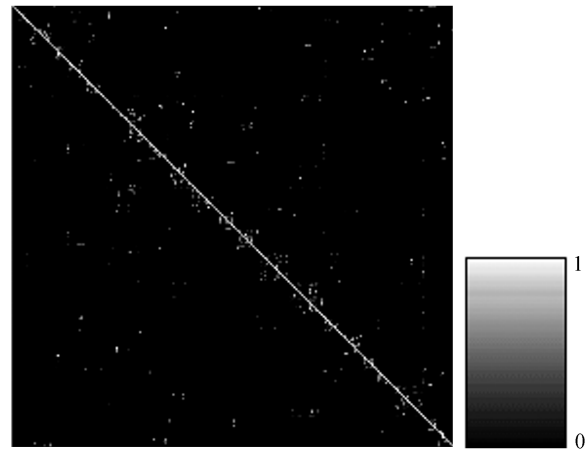

Fig. 5. The spatial interaction (connectivity) matrix constructed in GIS with data from a DEM and village boundaries. This matrix has 227 rows and 227 columns.

4 Snail density estimation with remote sensing

Previous research involving remote sensing for schistosomiasis control primarily concentrated on the mapping of potential snail habitats. Xu *et al*.[14] attempted to construct a statistical relationship between field survey snail densities and land cover information derived from remote sensing data, producing a snail density for the entire study area. They used a 4-m resolution IKONOS multispectral imagery and a DEM derived from ASTER images, spatially densified into 4 m grids in a land cover classification. As a result, 16 land cover types were obtained (Fig. 6). Field validation indicates that the average accuracy of this map is 89%. Classification accuracies of the major cover types such as residential areas, flood plains, crop areas, riverbeds, lowland terraces, high land terraces, and forest areas are all greater than 87%. The land cover types are intentionally schemed so that they are not sensitive to season. In this manner, it is possible to establish statistical relations with imagery obtained from different seasons for snail density estimation. In order to find out if detailed land cover information with such a classification scheme can be derived from remote sensing data at lower resolutions, the land cover data derived from the 4-m data were converted to fractional cover data based on an aggregation of 7×7 pixels. We then applied a linear model to estimate snail density,

$$\widehat{SA} = \widehat{a_1} f_1 + \widehat{a_2} f_2 + L\widehat{a_i} f_i L + \widehat{a_k} f_k, \quad (7)$$

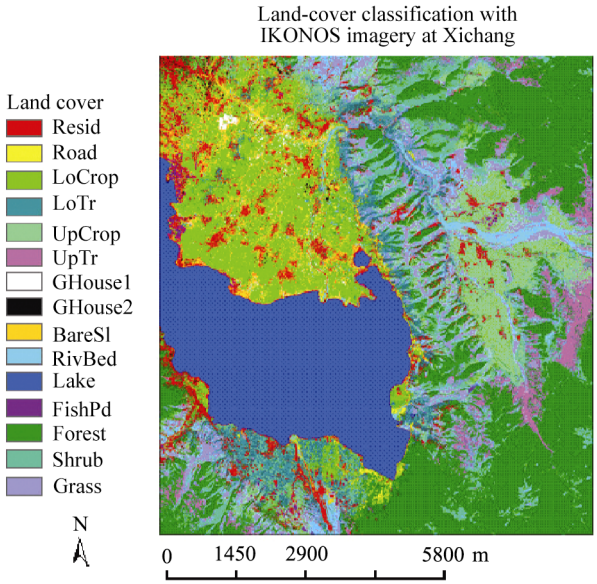

Fig. 6. Land cover map of the Xichang area based on IKONOS and DEM data.

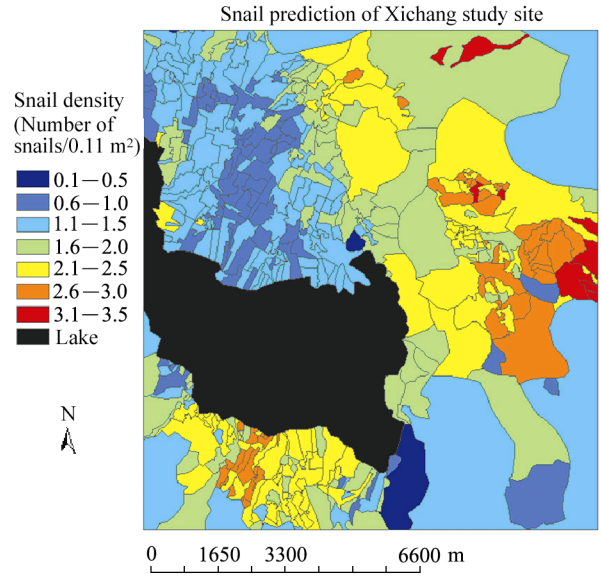

Fig. 7. Snail density map of the study area estimated with land cover fraction data.

where f is the fraction of area for a particular land cover type calculated from the 7×7 pixel window; SA is the estimated snail density; and a's are the coefficients of the model. The snail density for each village was calculated. Using over 10,000 snail sampling points collected in the ditches from 19 villages, they found that the R^2 value between survey data and the estimation data could be as high as 0.87.

Because it is very time and labor intensive for snail surveys in the field, we only did field surveys in the summer of 2001. We surveyed 19 villages for every ditch at 10 m intervals. At each sampling site, we placed a Kuang (0.11 m^2) to survey the snail density. A shortcoming of this experiment was that we did not have independent samples to validate our statistical model, since we used all the sampling data when building the multivariate statistical model in eq. (7). Additionally, snail density changes with season. Another shortcoming of this research was that we did not use satellite data from multiple times to estimate snail density variation in time. However, since the purpose of this study is mainly to test the feasibility of the conceptual model for spatial temporal dynamics simulation, this is sufficient. With eq. (7), we can calculate the snail density for each village. By then using the village area, the snail number in each village can be obtained (Fig. 7). Snail number can then be applied in eq.(4).

5 Simulation results

Based on model parameter adjustments, we used eqs. (1)—(5) to simulate the schistosomiasis transmission dynamics. With spatial connectivity, our temporal dynamics model became a spatial temporal model. We tested the model from June 15, 2000 and ran it on a daily basis for 5 years. The worm load in year 1 and year 5 is shown in Fig. 8. Clearly, if there is no schistosomiasis control the worm load increases annually. The areas showing no change are forested areas with no human settlement. The total number of simulated worm load after 5 years is 789467.

The effect of schistosomiasis control is easy to examine with the spatial temporal model. If only the patients in 5 villages can be treated for 1 week, our model can help us to answer which villages should be selected to maximize the control effect. For example, we can select the villages with the greatest worm load for treatment. Or, we can select the villages with the strongest spatial connectivity. We can also consider both, that is, those villages with high worm load and also high connectivity with a large number of effective neighbors. Fig. 9 compares two treatment plans: treating the 5 villages with the greatest worm load and treating the 5 villages with high worm load and high spatial connectivity. Treating the 5 villages with the greatest worm load caused a reduction of 13211

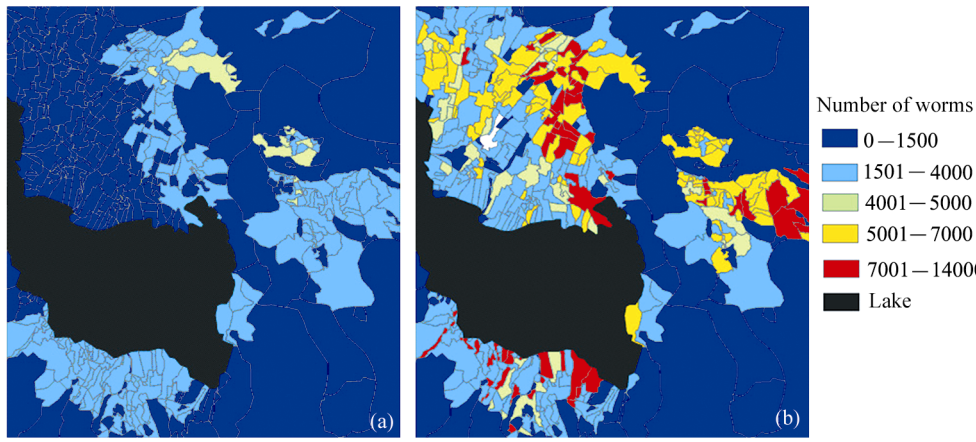

Fig. 8. Worm load in each village as simulated with the spatial temporal model. (a) Model simulation results for the first year and (b) model simulation results for the fifth year.

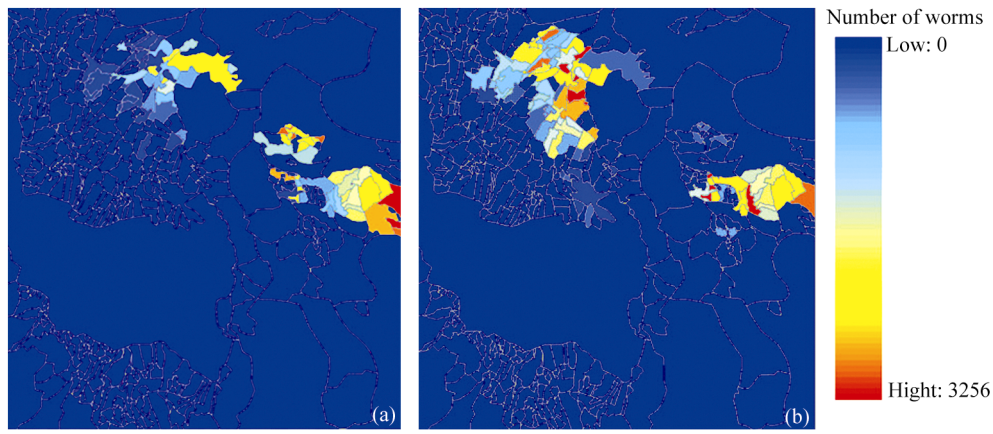

Fig. 9. Simulation results from the spatio-temporal model treating patients in 5 villages for one week each year. Two different village selection plans were compared: worm load reduction resulting from (a) treating 5 villages with the greatest worm load, and from (b) treating 5 villages with high worm load and high spatial connectivity.

worms, while treating the 5 villages with both high worm loading and high spatial connectivity led to a worm load reduction of 17505. From Fig. 9, the influence of the later treatment plan can reach many more villages. Therefore, it is necessary to compare different control strategies by considering spatial connectivity. The advantage of this spatio-temporal model for schistosmiasis transmission and control is that it allows us to develop and compare various control plans, in order to select the optimal ones to support control decision making.

Figure 10 compares the simulation results without schistosomiasis control to results with the patient treatment from the second village selection plan. Only the cercaria number and worm load are shown in the figure. Each curve represents results for one village in the 5 year simulation period. There is a clear distinction between the two simulations for cercaria production and worm loading in each village. Because treating 5 villages primarily kills the worm in hosts, some of the worm load drops in the curves can be clearly seen in Fig. 10(d).

The simulation results for cercaria production (Fig. 10(c) and worm loading (Fig. 10(d), based on the spatial temporal model with a control plan of treating patients in 5 villages that have high worm load and high spatial connectivity.

6 Summary and discussions

The above results demonstrate

(1) The conceptual model for the spatio-temporal

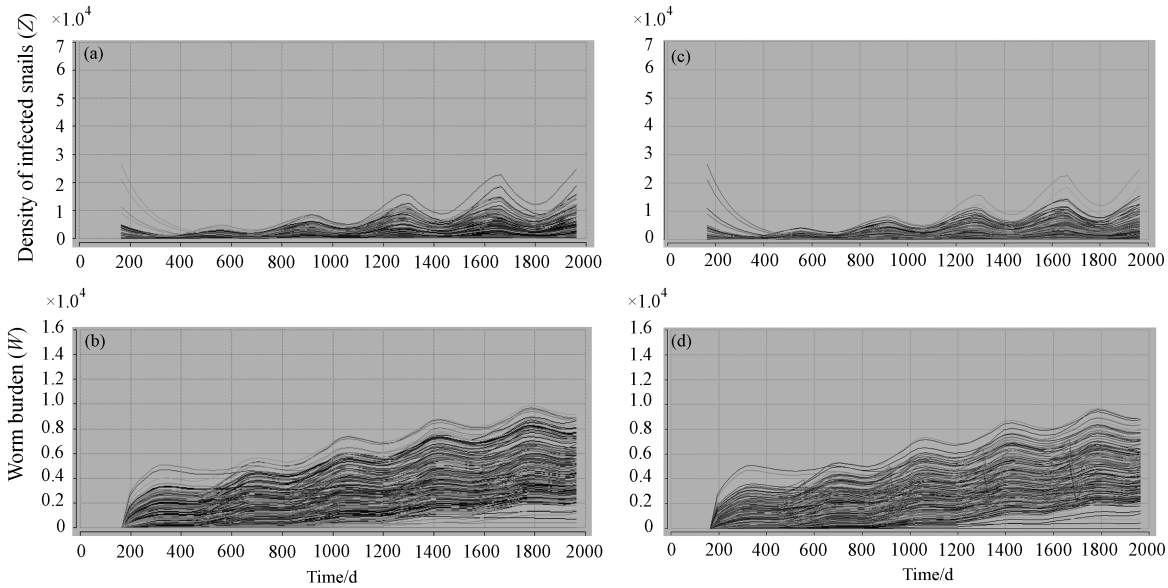

Fig. 10. The simulation results for (a), (c) cercaria production and (b), (d) worm loading, based on the spatio-temporal model without any control.

schistosomiasis transmission dynamics can be realized.

(2) Remote sensing and geographic information system are indispensable components in such spatio-temporal models.

(3) It is possible to use a spatio-temporal schistosomiasis transmission model in supporting spatial decisions, to improve the effectiveness of schistosomiasis control.

However, much work needs to be done to build a practical model. Firstly, we need to further investigate snail density estimation methods based on remotely sensed data from multiple sources. Secondly, spatial connectivity exists at multiple scales and among different environmental factors, and more work needs to be done in this aspect. For example, the spatial unit in this study is natural villages; but, populations can be divided at even finer units, such as at the occupational level, family level, or even at the individual level. On the other hand, scaling up from the village unit to the township and county level still remains to be resolved. Thirdly, more field data need to be collected to validate the models developed.

The transmission of schistosomiasis only represents one type of transmission processes for an infectious disease interacting with vectors, intermediate host and various environmental factors. Each infectious disease has its original endemic area. Its spatial transmission mainly relies on the natural forces, such as climate variation, vegetation succession, atmospheric and ocean circulation. Human activity promotes the transmission of infectious disease to new environments, by facilitating species invasion. Thus, human activity in the infectious disease transmission system acts as a positive feedback. We must have a better understanding of this positive feedback system, establish a better prediction model, and improve our prevention capacity. The model proposed in this study sheds lights on the spatio-temporal modeling of other infectious diseases. When the biological and environmental processes between the origin of the disease, its vector and host are relatively clear, we can adopt such models to predict the spatial and temporal dynamics of an infectious disease. For example, the plague, hemorrhagic fever with renal syndrome, and lyme disease can be modeled using the conceptual framework proposed here. Remote sensing and GIS can play important roles in supporting the spatial decisions in controlling infectious disease transmission.

Acknowledgements This work was partially supported by the National Natural Science Foundation of China (Grant No. 30590370), the Tenth-Five-Year Key Project (Grant No. 2004BA718B06) and an NIH (Grant No. RO1-AI-43961). We are grateful to the research group led by Prof. Xueguang Gu and Dongchuan Qiu in Sichuan Institute of Parasitic Diseases of China, and to Prof. Bob Spear and Dr. Ed- mund

Seto from the School of Public Health at University of California Berkeley for their help in field work and data preparation.

References

1 Rogers D J, Randolph S E. Studying the global distribution of infectious diseases using GIS and RS. Nat Rev: Microbiol, 2003, 1: 231－237
2 Zhou Y, Maszle D, Gong P, et al. GIS based spatial network models of schistosomiasis infection. Geogr Info Sci, 1996, 2: 51－57
3 Spear R, Gong P, Seto E, et al. Remote sensing and GIS for schistosomiasis control in mountainous areas in Sichuan. China Geogr Info Sci, 1998, 4: 14－22
4 Anderson R M, May R M, Anderson B. Infectious Diseases of Humans: Dynamics and Control. London: Oxford University Press, 1991
5 Liang S, Mazsle D, Spear R. A quantitative framework for a multigroup model of *Schistosomiasis japonicum* transmission dynamics and control in Sichuan. China Acta Trop, 2002, 82: 263－277
6 Hubbard A, Liang S, Maszle D, et al. Estimating the distribution of worm burden and egg excretion of *Schistosoma japonicum* by risk group in Sichuan Province. China Parasitol, 2002, 125: 221－231
7 Zhao W X, Gu X G, Xu F S, et al. An ecological observation of Oncomelania hupensis robertsoni in Xichang, Daliang Mountains, Sichuan. Sichuan J Zool (in Chinese), 1995, 14(3): 119－121
8 Xie F X, Yin G L, Wu J Z, et al. Life span and cercaria shedding of schistosome-infected snails in mountainous region of Yunnan. Chin J Parasitol Parasit Diseases (in Chinese), 1990, 8(1): 4－7
9 Stelma F F, Talia I, Sow Set al. Efficacy of and side effects of praziquantel in an epidemic focus of *Schistosoma mansoni*. Am J Trop Med Hyg, 1995, 53: 167－170
10 Liang Y S, Coles G C, Doenhoff M J. Short communication: Detection of praziquantel resistance in schistosomes. Trop Med Int Health, 2000, 5(1): 72－72
11 Pesigan T P, Hairston N G, Jauregui J J, et al. Studies on *Schistosoma japonicum* infection in the Philippines. 2. The molluscan host. Bull WHO, 1958, 18(4): 481－578
12 Qian B Z, Qian J, Xu D M, et al. The population dy- namics of cercariae of Schistosoma japonicum in *Oncomelania hupensis*. Southeast Asian J Trop Med Public Health, 1997, 28(2): 296－302
13 Xu B, Gong P, Seto E, et al. A spatial-temporal model for assessing the effects of inter-village connectivity in schistosomiasis transmission. Ann AAG, 2006, 96(1): 31－46
14 Xu B, Gong P, Biging G, et al. Snail density prediction for schistosomiasis control using IKONOS and ASTER images. Photo Eng Remote Sensing, 2004, 70(11): 1285－1294